

Application of G. Lamé's and J. Gielis' formulas for description of shells superplastic forming

*Aleksandr Anishchenko*¹, *Volodymyr Kukhar*¹, *Viktor Artiukh*^{2,*} and *Olga Arkhipova*³

¹Pryazovskyi State Technical University, Universytetska, 7, Mariupol, 87555, Ukraine

²Peter the Great St. Petersburg Polytechnic University, Polytechnicheskaya, 29, St. Petersburg, 195251, Russia

³Tyumen Industrial University, Volodarskogo str., 38, Tyumen, 625000, Russia

Abstract. The paper shows that the contour of a sheet blank at all stages of superplastic forming can be described by application of the universal equations known as a "superformula" and "superellipse". The work provides information on the ranges of values of the coefficients entering these equations and shows that their magnitudes make it possible to additionally determine the level of superplastic properties of the workpiece metal, the shape of the shell being manufactured, the stage of superplastic forming, and the presence of additional operations to regulate the flow of the deformable metal. The paper has the results of approximation by the proposed equations of shell contours that manufactured by superplastic forming by different methods.

1 Introduction

Superplastic forming (SPF) of casings of hemisphere type, spherical shells, boxes, box sections and the like of sheet blanks is a relatively new technological process of plastic working of metals, that sprang up owing to discovery of the phenomenon of superplasticity in metals and alloys. SPF was first copied in 1964 from the process of gas forming of thermoplastics [1, 2]. Some of the materials developed for superplastic forming are known [2]: Aluminium-Magnesium (Al-Mg) alloys, Bismuth-Tin (Bi-Sn), Aluminium-Lithium (Al-Li), Zinc-Aluminium (Zn-Al) alloys, URANUS 45N (UR 45N) two phase stainless steel, Nickel (Ni) alloy INCONEL-718, Titanium (Ti-6Al-N) and Pb-Sn alloys. For such technique a flat sheet blank is placed into a sealed die-container, then the blank is fixed (clamped), according to the required shape and subsequently formed by free bulging (Fig. 1a) or by blow forming (Fig. 1b) by means of supply of pressurized gas energy carrier [3-5]. This provides this process with additional low-tooling advantages.

Constant growth in parts and materials range, manufactured by SPF of sheets, including in combination with diffusion welding [2, 3] stipulates the necessity to modify the existing methods and develop new ones for designing of these processes. For a control over the processes of forming, evaluating of the parameters of the deflected mode and designing of the elements of die tooling it is required to predict and describe the changing shapes of sheet blanks formed by application of SPF methods. Nowadays an active search is going on

* Corresponding author: artiukh@mail.ru

for precise mathematical methods of describing bodies shapes and forming at a different stage of impression-free and dieless methods of sheet and bulk workpieces performing [4-8]. Possibilities of new mathematical discoveries in the field of approximate description of any existing natural contours make it possible to apply Lamé's [9-10] and Gielis' [11-13] formulas, as they seem to be very perspective. Such investigations have not been carried out yet, it ensuring scientific novelty of the work.

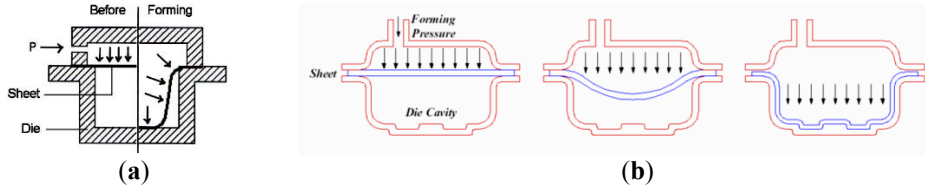


Fig. 1. Superplastic methods of sheet blank forming: (a) – free bulging, (b) – blow forming

The processes of superplastic forming of hollow parts, manufactured of sheets (see Fig. 2) are calculated, as a rule, on the basis of the thin-walled moment-free (membrane) shell theory with application of Laplace's equation [14-17]:

$$\frac{\sigma_1}{R_1} + \frac{\sigma_2}{R_2} = \frac{p}{S}, \quad (1)$$

where σ_1, σ_2 – meridional and tangential stresses inside the shell at forming;

R_1, R_2 – radii of the shell's curvature in the meridional and tangential directions;

p – pressure of the deforming environ;

S – thickness of a sheet blank.

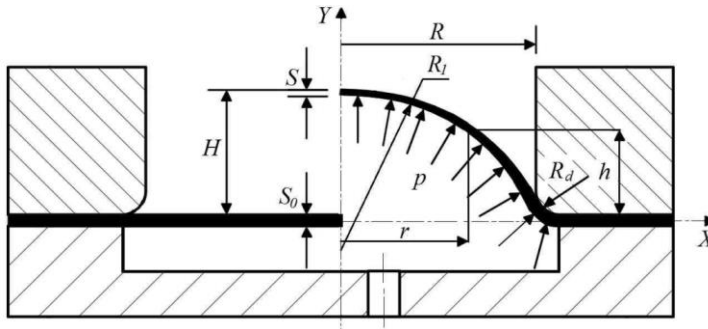


Fig. 2. The design scheme of the superplastic forming process

As a coupling equation the equation of steady creepage is most often used [5, 17-21]:

$$\sigma = k\xi^t, \quad (2)$$

where σ – intensity of flow stresses;

k – material's properties index;

ξ – intensity of strain rates;

t – strain rate hardening exponent (is an sensitivity index to evaluate the dependence of flow stress σ on strain rate ξ).

At least two stages of forming [3-5, 19] are considered for SPF calculations: 1) free bulging of the initial blank into the die-cavity to the contact with its bottom, 2) filling of

angular areas of die for shells or boxes with the deformed metal. Sometimes, the forming of the triangular sections of the box-parts or the formation of rigidity ribs on the parts' surface is singled out as the third stage [22], compensating elements often being used for improving of parts geometric precision [23, 24]. The need of stage-by-stage calculation of SFP process is caused, above all, due to essential alternations of the contour's geometry of the deformed blank part at its passing from die forming to flowing into the corner areas of mating first on the bottom and side surfaces of shells and boxes and then into trihedral corners of the boxes or into the hollow parts of rigidity ribs. Besides, contact friction conditions are changed on the blank-die boundary [25].

The non-monotonous evolution of the contour of a blank sheet at SPF causes drastic alternations in the radii of curvature R_1 and R_2 , it complicating calculations according to Laplace's equation (1). The radii of curvature R_1 and R_2 are usually determined by approximating experimental data with different formulas. For the first stage of SPF it is often assumed that the contour of the formed blank is but a part of the circumference [1], seldom it has a parabolic shape [18] or an ellipse shape [26, 27]. For calculations of the corner areas parts of the contour are approximated by circumferential equations [1, 4], using polynomials and splines (equations of a chain line and circumference) [8, 28]. For evaluations of SPF technology transition from one stage to another is very often due to alternation of the system of coordinates, original assumptions, boundary conditions and the absence of interconnectivity of the indices comprising the equation (2). It makes the calculations more complicated, reducing their precision, it being in spite of all another prerequisite for application of Lamé's [9, 10] and Gielis' [11-13] formulas for solution of the problems of approximating the formed blanks' contours.

A number of researchers [5, 18] assume that the shape of blank's contour at SPF depends upon strain rate hardening exponent t : the bigger t -index value the closer the contour of the blank is to circumferential shape. They believe that low level of superplasticity properties of blank's metal, i.e. low values of t , determine transition of the contour from circle to parabolic or even hyperbolic shape [29].

Still, we maintain that predicting the blank's shape at SFP, on the basis of the value of t -index is incorrect. The value of t -index is determined in connection with the entire specimen under testing. In case with SFP blanks with changed structure of separate sections and forming. In case with SPF blanks with altered structure of some sections and when forming is done within an uneven temperature field it is a normal practice to try to achieve reduced or increased parameters of superplasticity of the deformed method inside the specified areas [17, 29]. If t -index is evaluated for such conditions of deformation it will be essentially less than its optimal value, according to which a geometric shape of the deformed blank is supposed to be evaluated. Due to it the contour of the crown differs from spherical shape of the sheet part, manufactured by forming [1, 17, 28-30], and the blank temperature along the crown's pole is reduced, as compared to the optimal value. According to the works [26, 27, 31]: a) the contour of a titanium tube with a coarsened structure in the central area during superplastic expanding or flaring is closer to the bellows contour than to a circle or parabola; b) crowns (domes) during SPF of blanks with grinded grains on a some circle sector of their diameter had a contour similar to a peeled orange.

As far as SPF blanks of different thickness are concerned [38, 39], the crown shape at the same value of t -index for all sections of the blank may change both to parabolic and ellipse type. It depends on the locations of sections with maximal and minimal thickness on the blank's surface and the difference between these thicknesses in relation to the average thickness of the blank the analysis of t -index, described, for instance in [1, 4, 5, 31, 32] shows that its numerical values are not constant and depend on many factors, so it cannot be considered as an objective criterion for evaluating SPF parameters.

According to our opinion the conclusions of the authors of [3, 5, 6, 19, 20, 32-34] works seem to be relevant, when they ascertain that the shape of the contour (profile) of a deformed blank part depends on distribution of its relative thickness. It can be explained by the following reasons:

1) it was found experimentally [3, 19, 20, 32, 34], that for smith SPF the maximum deviation of the crown's shape from spherical shape was observed at the smallest values of S/S_0 in the crown's pole (S, S_0 – are the current and initial thicknesses of the sheet blank);

2) prior to fracturing of the crown's walls, a local bulging of the crown with abnormal decrease in the radius of curvature takes place, simultaneously with a drastic decrease of the blank's thickness, this phenomenon is typical to both superplastic and ordinary cold forming of parts, like, for instance, by liquid pressing [2, 3];

3) adjusting the blank's thinning (as a rule, reduction of difference in thicknesses of its walls) by SPF methods of variable thickness, by preliminary preparation of different structures in the specified sections and in an even temperature field is accompanied with an evident deviation of the crown at the stage of smith forming, from the shape of spheroid segment [1, 17, 29, 30, 38-40].

The performed review shows the vitality of finding ways of approximation of contours of sheet blanks at superplastic forming, by application of a unified equation, for the sake of unifying the approaches to a detailed analysis of shape alternation and tools' contours design in order to ensure their standard durability [35, 36].

The objective of this work is to determine the possibility of approximating the contour of a forming blank by a single unified equation at all SPF stages, with due regard to ever changing geometrical and technological parameters.

2 Methodology

For selection of a universal equation for description of shells' contours, formed under conditions of superplasticity it should be noted that its diagrams must describe different shapes of parabolas, circumferences, and rectangles with rounded angles, at different values of parameters, comprising it.

We assume that such equations may comprise an equation of Gabriel Lamé's curve, more widely known as a "superellipse" [9, 10], and Johan Gielis' equation [11-13], known also a "superformula".

The "superellipse" is generally described in Cartesian coordinated with the following equation:

$$\left(\frac{x}{a_0}\right)^n + \left(\frac{y}{b_0}\right)^m = 1, \quad (3)$$

where n and m – exponents;

a_0 and b_0 – coefficients, $a_0 > 0$, $b_0 > 0$.

Depending on the values of n , m , a_0 and b_0 diagrams of the equation (3) describe the entire set of contours, that sheet blanks may have at different SPF stages.

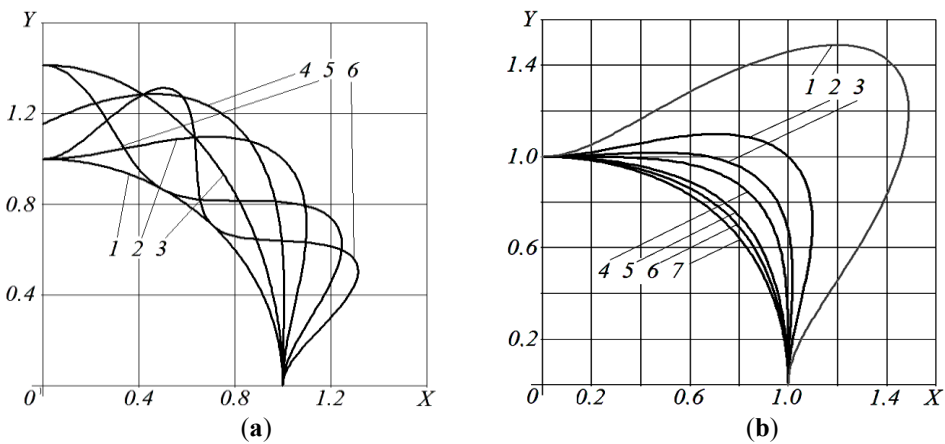
Johan Gielis offered in his classical work [11] a more generalized equation, known nowadays a "superformula", it may be applied for describing many complicated shapes and curves, that are met in nature and engineering [12-13]. In geometrically opposite coordinates for radius-vector r and φ angle the equation has the following view:

$$r = \frac{1}{\sqrt[n_1]{\left[\frac{1}{a} \cos\left(\frac{k}{4}\varphi\right)\right]^{n_2} + \left[\frac{1}{b} \sin\left(\frac{k}{4}\varphi\right)\right]^{n_3}}}, \tag{4}$$

where n_1, n_2, n_3 – curve’s shape indices;
 a, b – dimensions (values of semi-axes);
 k – index of the number of repeated fragments.

The authors rightfully consider the equation (4) to be a new way of describing and represented natural objects and maintain that the variety of shapes can be described with one singular and simple numeric equation. The circumferential equation, reduced to more general view and having acquired the view of (4) equation can form lots of generations of different curves and polygons, including shells’ contours at SPF.

Now, let us consider the graphs of the “superformula” (4), its parameters n and m are changed within 1...24 limits (see Fig. 3). Lamé’s superellipse (3) is its particular case ($n_1 = n_2 = n_3 = k = 4$) and it represents a rectangle with rounded angles. As the sought values at shells SFP are normally investigated in non-dimensional parameters (with regard to the highest values of the initial blank’s thickness S_0 , the radius of the shell’s base R , the final height of the shell H , etc.) of interest to us, first and foremost, there will be graph’s sections within $0 \leq x \leq 1$ and $0 \leq y \leq 1$ intervals. To do it we’ll assume $x = X = r/R$, $y = Y = h/R$, $a = R/R = 1$, $b = H/R = 1$, where r and h – current values of the radius of the base (cap) and the height of the shell, respectively for (4) equation. The graphs, situated in the first quadrant of the coordinate plane may be expressed in other quadrants symmetrically with regard to the coordinate axes.



- (a): 1 – $k = 4, n_1 = n_2 = n_3 = 2$;
- 2 – $k = 4, n_1 = n_2 = 4, n_3 = 2$;
- 3 – $k = 2, n_1 = n_2 = 4, n_3 = 2$;
- 4 – $k = 3, n_1 = n_2 = 4, n_3 = 2$;
- 5 – $k = 6, n_1 = n_2 = 4, n_3 = 2$;
- 6 – $k = 8, n_1 = n_2 = 4, n_3 = 2$

- (b): 1 – $k = n_1 = n_2 = 4, n_3 = 1$;
- 2 – $k = n_1 = n_2 = 4, n_3 = 2$;
- 3 – $k = n_1 = n_2 = 4, n_3 = 3$;
- 4 – $k = n_1 = n_2 = 4, n_3 = 4$;
- 5 – $k = n_1 = n_2 = 4, n_3 = 8$;
- 6 – $k = n_1 = n_2 = 4, n_3 = 12$;
- 7 – $k = n_1 = n_2 = 4, n_3 = 24$

Fig. 3. Superformula graphs at $a = b = 1$ and different values of n_1, n_2, n_3, k parameters

Fig. 3a shows what additional possibilities can be revealed in Gielis’ superformula in comparison with Lamé’s superellipse by introducing into it $(k/4)$ multiplier. Only curve 1

which parameters characterize it as a circle at $(k/4)=1$ or $(k=4)$ is inscribed in the coordinate area restricted by $0 \leq x \leq 1$ and $0 \leq y \leq 1$ boundaries. In other cases superformula's graphs exceed the above-mentioned bounds, showing their periodicity, typical of trigonometric equations, which comprise the superformula. With regard to symmetry of graphs on relation to the coordinate axes, the number of periods in the first quadrant of Cartesian coordinates is determined by the value of $(k/4)$. At $(k/4) = 2$ (the same $k = 8$) there will be 2 (see 6 curve) at $(k/4) = 1,5$ or $(k=6)$ and one period and a half (curve 5), etc.

Thus, introduction of the parameter of $(k/4)$ into the equation (4) allows overcoming the main disadvantage of "superellipses" – their limitations in symmetry. If k -parameter is available the plane may be divided into a multitude of sectors, their number is equal to k instead of four quadrants in Euclidean plane. For example, at $k = 3, 4, 5 \dots N$ is curve which described in four quadrants by means of equation (4) will have 3, 4, 5... N number of repeated fragments.

The higher the level of symmetry of analyzed contours the simpler view the superformula (4) acquires, as the indices $n_1..n_3$, and in some cases the values of a and b semi-axes become equal to each other. Because of it, bearing in mind the objective of our work, the multiplier $(k/4)=1$ or $(k=4)$ should have been used in the superformula.

Fig. 3b represents the evolution of graphs of the superformula at different values of n_3 parameter. An essential change in the curvature of graphs 1 – 3 and their retreat from the beginning of the coordinates at $n_3 < 4$ is the reason for their unfitness for approximation of shells' contours at SPF. If $n_3 \geq 4$, then graphs' appearance is qualitatively changed, same as at similar changes at n and m in Lamé's superellipse, in condition that $n = m$.

Thus, if approximation of most common shells' contours formed in the superplastic state from sheets is the case, when one or several planes of symmetry are present (spheres, cylindrical shells, round and square boxes) both equations (3) and (4) are applicable. The approximation by Lamé's superellipse seems to be easier, as it requires determination of numerical values of two coefficients n and m only. More intricate shells' contours (boxes equipped with rigidity ribs, cylindrical shells with undercuts, ogives, having surfaces with different curvature radii, etc.) should be approximated by Gielis' "superformula".

3 Result and discussion

Now, let us analyze the possibilities of describing shells' contours by means of Lamé's superellipses (see Fig. 4). The analysis of the graphs shows that the equation (3), in which $n \leq 1$ at all values of m from 0.25...8 interval are inapplicable for approximation. Even at $m = 4$ and $m = 8$ the graphs (Fig. 4a) in the point with $x = 0$, $y = 1$ coordinates have the inclination angle to x axis, not equal to zero, it being impossible both in case of crowns formation and for SFP of shells and boxes. The curves of the equation (3) (see Fig. 4b) at $n = 2$ and $m \geq 1$ could be, in principle applied for approximation of both parabolic and ellipse-like contours of shells at the first SFP stage and also for description of formed contours and shells at the second stage of SPF.

The graphs of the "superellipses" in Fig. 4c at $n = 4$ can be used approximation of several variants of shells' contours. At $m \geq 1$ values graphs 3-6 simulate the contour of the shells, the crown of which has reached the die bottom and the second SFP stage has begun. At $n = m = 4$ the angular areas are formed with equal strain of the polar and flange areas of the shells, at $m = 1$ and 2 it happens with prevailing of thin polar areas, at $m = 8$ – at

deceleration of shell's deformation in the polar areas by when frictional forces rub against the die and the shell's angular areas are formed mainly by means of thinning blank's section, located near the flanges.

The curves 1 and 2 ($m = 0.25$ and 0.5) in the point with $x = 1$, $y = 0$ coordinates have some overbending, it allowing their application for approximation of shells' contours with due regard to the radius of rounding of the die.

It is shown in Fig. 4d that by applying of the superellipse at $n = 8$ it is possible to simulate the contour of shells, forming angular areas, mainly, due to deformation of the central sections of the shell. At $n = m = 8$ deformation of the polar and flange areas of the shell is nearly the same, while the radius of rounding of the angular area is essentially less, than for the curve with $n = m = 4$. Curves 1 and 2 ($m = 0.25$ and 0.5) have an overbending in the point with $x = 1$, $y = 0$ coordinates, like Fig. 4c, although their radius is smaller so they can express the shells' contour with and without the rounding radius of the die.

The advantage of the analyzed equation is its possibility to determine by means of the value of coefficients, described above, the contour of the manufactured part and, hence, the stage of SPF, which the "superformula" describes, as well as the presence of superplasticity properties of deformed metal. In mathematics a parameter of rectangularity $\eta = 2/n$ (here is $n = m$) is introduced for these purposes. The closer to one the value of η is, the closer to circumferential shape the contour of the deformed part is at the stage of blow molding, i.e. the bigger is the level of superplasticity properties of deformed metal.

The values $2 > \eta > 1$ testify a low level of blank's metal superplasticity, and transition of its spherical contour (in the first two quadrants of the crossing plane, i.e. at positive ordinates) into parabolic and then up to conical (at $\eta = 2$ and $n = m = 1$), that can take place at filling of rigidity ribs with a triangular contour in section. In all four quadrants the graph of the superformula has a shape of a rhombus, rectangle or a square with vertices on the coordinate axes.

At $4 > \eta > 2$ ($n < 1$ and $m < 1$) the superformula is gradually transformed into an astroid ($\eta = 4$). The values of n and m smaller than one testify errors, occurred, while approximating with the superformula.

The interval of $2 < (n, m) < 4$ or $1 > \eta > 0.5$ values gives us an opportunity to assume that the process of SFP is carried out with deceleration of deformation of the central areas of the blank. The contour of the blank is rearranged from spherical to elliptic. At $n = m = 4$ (the variant of the superformula is "superellipse" thoroughly investigated by Lamé) the curve's contour acquires a rectangular shape with quite an essential radius of sides coupling in the angles. It can be maintained that the superformula describes in this form the second stage of SPF – filling of the angular zones of cylindrical or box-shaped parts. The radius acceptable for parts of shell or box type in angles, equal to two-four thicknesses of the blank is reached at $(n \text{ and } m) = 7 \dots 10$.

Besides, if $n > m > 4$, then at the second stage of SPF deformation of the crown's central areas occurs, exceeding deformation in the blank's sections, close to flanges. It may occur if there is some efficient lubricant with low constant of friction between the bottom of the die and central areas of the crown. The shape of the semi-finished product is characterized by presence of flat polar surface, transferring into parabolic or hyperbolic surface of peripheral sections, which have no contacts with the side surface of the die.

The superformula with $m > n > 4$ is applicable if the blank before the SPF was subjected to a deep drawing by rigid punch (pneumomechanical forming). The graph of the superformula has a straight vertical section near the flange passing into an elliptical curve that ending in the pole of the crown.

Now, let us consider shells' geometrical shape at two stages of SPF: (a) – at $H = R$ (at the first stage and (b) – at $H = 0.6R$ (the next stage). We'll also consider the peculiarities of its approximation by Lamé's equation, using the data listed in [18, 32, 37]. As was mentioned before, the choice of the is explained by the presence of a big number of axes and planes, due to which application of more complicated Gielis' formula is hardly advisable.

For approximations of contours at $H = R$, the shells manufactured of *AlMg5* and *Sn-38 %Pb* alloy were chosen with different values of t -index, and of *AlMg6* [18, 32, 37] alloy also. Blanks, made of *AlMg6* alloy had a variable thickness: $S_0 = 1.45\text{mm}$ in the central part with a diameter of 60mm, and $S_0 = 1.23\text{mm}$ in a ring peripheral section with outside and inside diameters being of 100 and 60mm, respectively.

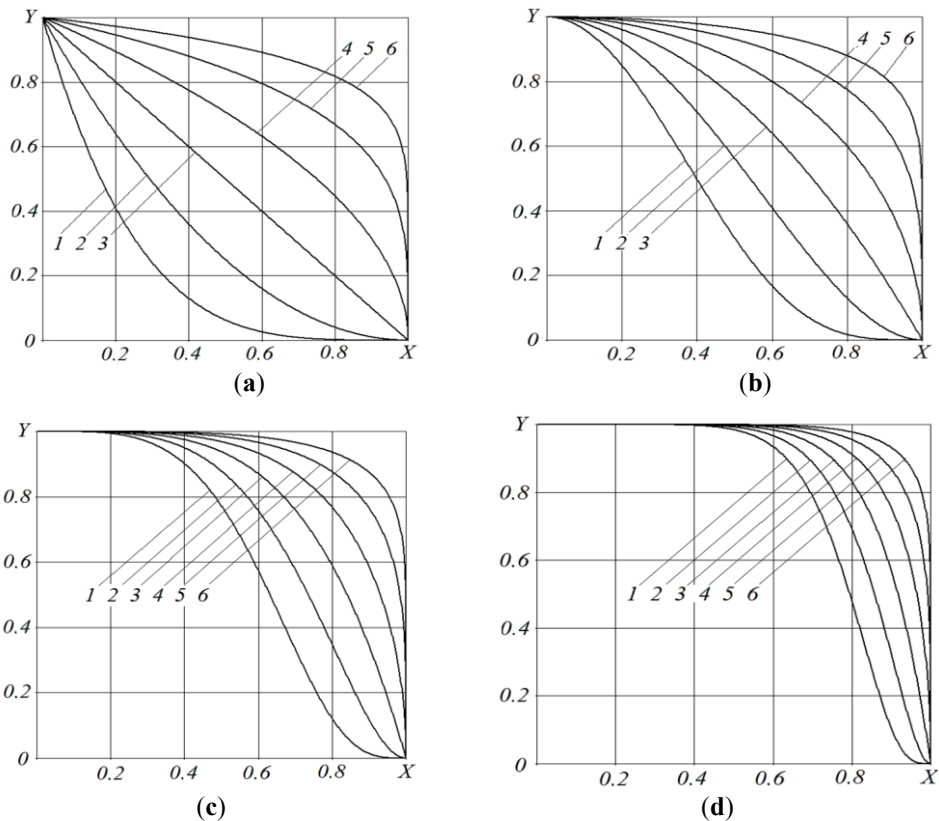


Fig. 4. Graphs of “superellipses” at $a = b = 1$ and different values of n and m parameters:

(a) – $n = 1$; (b) – $n = 2$; (c) – $n = 4$; (d) – $n = 8$;

1 – $m = 0.25$; 2 – $m = 0.5$; 3 – $m = 1$; 4 – $m = 2$; 5 – $m = 4$; 6 – $m = 8$

For approximation of contours at $H = 0.6R$, the shells manufactured of *AlMg3* [37] alloy were chosen, having the shape of: a) spherical-like segments, formed at the first SFP stage under isothermal conditions and in uneven temperature field; b) intermediate semi-finished shells, formed at the second SPF stage into a cylindrical die.

Table 1 represents Lamé's equations (after the transformations and simplifications) for approximating shells' contours at $H = R$ and $H = 0.6R$. Because many researchers [1-3] presume that a contour of a shell of small height at the initial stages of SPF has a shape of

spherical segment, it is expedient for further analysis of such assumption to define more exactly the types of equations of Lamé's superellipse for these cases.

Table 1. The equations of approximating of actual shells' contours at SPF

| For shells with $H = R$ | | For shells with $H = 0.6R$ | |
|---|---|--|--|
| Shell's parameters | Approximating equation in dimensionless view | Shell's parameters | Approximating equation in dimensionless view |
| <i>AlMg6</i> alloy, blank of variable thickness | $Y_{AlMg6} = \left(1 - X_R^{2.58}\right)^{0.51}$ | SPF of the segment in uneven temperature field | $Y_{TF} = 0.6\left(1 - X_{TF}^{2.36}\right)^{0.813}$ |
| <i>Sn-38 %Pb</i> alloy, $t = 0.6$ | $Y_{t0.6} = \left(1 - X_R^{2.02}\right)^{0.521}$ | Forming with shell's lubrication | $Y_L = 0.6\left(1 - X_L^{3.03}\right)^{0.756}$ |
| <i>Sn-38 %Pb</i> alloy, $t = 0,25$ | $Y_{t0.25} = \left(1 - X_R^{1.98}\right)^{0.581}$ | Forming without shell's lubrication | $Y_{NL} = 0.6\left(1 - X_{NL}^{2.58}\right)^{0.61}$ |
| <i>AlMg5</i> alloy | $Y_{AlMg5} = \left(1 - X_R^{1.99}\right)^{0.562}$ | Segment's SPF in isothermal conditions | $Y_P = 0.6\left(1 - X_P^{1.94}\right)^{0.781}$ |

The spherical segment formed at initial stages of blank's bulging has the contour approximated by circumferential equation:

$$\left(\frac{x}{R_k}\right)^2 + \left(\frac{y}{R_k}\right)^2 = 1, \quad (5)$$

where R_k – is the radius of the circumferential curvature, forming segment's contour with $2R$ chord and H height.

The radius R_k of curvature is related to the current height h and the radius R of segment's base (cap) by following ratio:

$$R_k = \frac{R^2 + h^2}{2h}. \quad (6)$$

Designating $h = \beta R$, we can write down the equation (5) in this view:

$$\left[\frac{2\beta x}{(1+\beta^2)R}\right]^2 + \left[\frac{2\beta y}{(1+\beta^2)h}\right]^2 = 1. \quad (7)$$

Let us transfer the beginning of coordinates for (7) equation to the point of intersection of height and base radius of the segment, i.e. at a distance along y -axis, equal to $(R_k - h)$, then, the equation (7) will acquire the following view:

$$y = h\left(\frac{1+\beta^2}{2\beta}\right)\left[1 - \left(\frac{2\beta x}{(1+\beta^2)R}\right)^2\right]^{1/2} - h\left(\frac{1-\beta^2}{2\beta}\right), \quad (8)$$

or in dimensionless view:

$$Y_{SG} = \left(\frac{1+\beta^2}{2\beta}\right)\left[1 - \left(\frac{2\beta X_{SG}}{(1+\beta^2)}\right)^2\right]^{1/2} - \left(\frac{1-\beta^2}{2\beta}\right). \quad (9)$$

Particularly for semi-spherical shell ($\beta = 1$, $R_k = h = R$) we'll have:

$$y = R \left[- \left(\frac{x}{R} \right)^2 \right]^{1/2} \text{ or } Y_0 = (1 - X_0^2)^{1/2}, \tag{10}$$

where $Y_0 = h/R$, $X_0 = r/R$ – are dimensionless coordinates of circumferential contour's points, changing within $0 \leq (r, h) \leq 1$ interval.

Relative deviations q of real contours of shells with $H = R$ and $H = 0.6R$ from semi-spheres' contours Y_0 and spherical segments Y_{SG} with the radius of the base (cap) R are presented in Fig. 5 and Fig. 6. The relative deviation was determined as $q = Y_i/Y_j$, where Y_i – are approximating functions of real contours of shells (see Table 1); Y_j – circumferential equations Y_0 (10) and equations of the spherical segment Y_{SG} (9). All equations do not take into account the presence of the radius R_d of conjugation of deformable shell and the flange, i.e. they are not true within $r = (0.95...1.0)R$ interval.

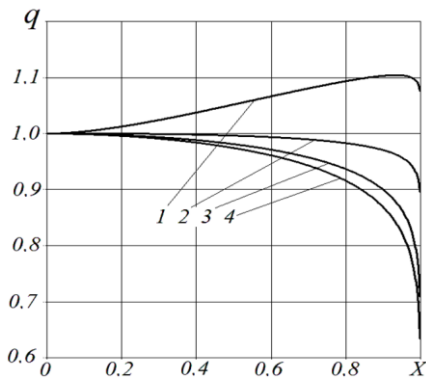


Fig. 5. Distribution of the relation of ordinates of shells' contours at $H = R$ and a semi-sphere along the radius of base (cap):

- 1 – $q = Y_{AlMg6}/Y_0$; 2 – $q = Y_{0.6}/Y_0$;
- 3 – $q = Y_{AlMg3}/Y_0$; 4 – $q = Y_{0.25}/Y_0$

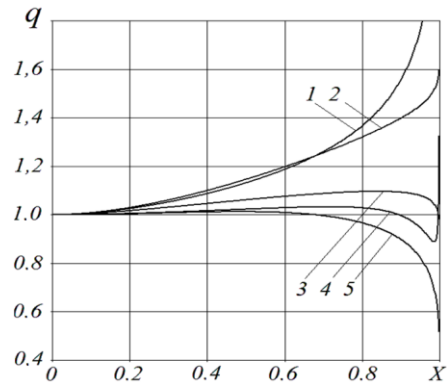


Fig. 6. Distribution of the relation of ordinates of shells' contours at $H = 0.6R$, made of *AlMg3* alloy along the radius of base (cap):

- 1 – $q = Y_{NL}/Y_P$; 2 – $q = Y_L/Y_P$; 3 – $q = Y_{TF}/Y_P$;
- 4 – $q = Y_0/Y_P$; 5 – $q = Y_L/Y_{NL}$;

Curves 2-4 of Fig. 5 confirm the data of researchers [18, 29, 37] that the contour of the shells molded free in the die-cavity is determined by the level of superplasticity properties of material. The smaller it is (small t -index value, greater multi-thickness of shells') the bigger is the deviation of the contour from spherical shape towards parabola. At that in the equations of approximation we have $m < n < 2$. However, if a blank of variable thickness is used for the SPF, the resulting change in the stress state will cause the displacing of the shell contour in central zones at the initial stage of the SPF toward the ellipse view (curve 1, Fig. 5). The approximation function Y_{AlMg6} is characterized here by $n > 2$ index, while $m < 2$, it being possibly caused by low of superplasticity properties of *AlMg6* alloy.

As can be seen from the graphs in Fig.6, parabolic shape of shell also occurs at its lower height $H = 0.6R$ (curve 4). Deviation q does not exceed 0.03 here within a reliable interval of change, while for shells with $H = R$ the q -parameter is within 0.04...0.18 intervals.

The chilling of a blank by water droplets falling from hodograph at 20 seconds interval upon the polar areas ensured uneven temperature field along the shell's contour at its forming during the initial stage of SPF. As a result of deceleration of thinning of central

shells' areas, its contour within the areas of the pole deviated from spherical shape towards ellipse, just like in case with application of a blank with variable thickness (see curve 3, Fig.6). The maximum ratio of the ordinates of the approximating equation Y_{TF} and Y_P was $q_{max} = 1.1$ at $X = 0.84$. Because of chilling of the central surface of the deformed blank it was not possible to mold the high crowns. Breakage of crown's walls was registered not in the pole, but in sections of the surface between the pole and the flange, and walls thickness in the polar areas was approximately equal to the thickness of walls in sections where metal breakage was observed.

The second stage of SPF at forming of a cylindrical shell with $H = 0.6R$ produces a contour of semi-finished product essentially dependant on presence of lubrication on the bottom surface of the die changing the character of metal flow at filling of the shells' angles.

At forming without lubrication the shell's sections which are in contact with the bottom of die are not deformed nearly and shell's contours are formed due to thinning of free zones of the shell. Presence of lubrication of "shell-bottom" boundary causes further thinning of polar areas at the second stage of SPF [4, 20, 37]. The contour of semi-finished product acquires a straight area originating in the pole of the crown and eventually passing to a parabolic curve propagating along the radius of conjugation of the die into the blank's flange. The straight area of the contour eventually grows bigger (the radius of shell's curvature increases) while such straight section of the contour appears later. The shell's ordinates in these areas are increased in direction of the bottom of the die with higher intensity, as compared to forming without lubricating (see curves 1 and 2, Fig. 6). Meanwhile, deformation of the areas near flanges is more intense at forming without lubrication. The curve 5 (Fig. 6) shows that within $0 < r/R < 0.68$ interval the ordinates of shell's semi-finished product are higher at SPF with lubrication, while the opposite state can be seen at areas near flanges.

4 Conclusions

The contours of a sheet blank at all stages of superplastic forming can be approximated by curves of universal equations known to be a "superformula", or "superellipse". The values of indices this equations comprises allow describing the superplastic metal properties of a blank at a qualitative level, as well as the shape of this blank, the stages of plastic-forming and presence of additional operation for regulation of the flow of deformed metal. Geometrical contour of shells at the initial SPF stage can vary from spherical to parabolic or ellipsoid. Presence of lubrication between the die and shell promotes an increase of the curvature radius in these sections at the second stage of SPF.

References

1. G. Giuliano, *Superplastic Forming of Advanced Metallic Materials: Method and Applications* (Oxford-Cambridge-Philadelfia-New Dehli, Woodhead Publishing Ltd, 2011)
2. P. K. Bhojar, International Journal For Administration in Management, Commerce and Economics (IJAMCE), 284-289 (2015)
3. V.A. Golenkov, A.M. Dmitriev, V.D. Kukhar, et.al., *Special technological processes and pressure treatment equipment* (Moscow, Mashinostroenie, 2004), in russ.
4. M. Balasubramanian, K. Ramanathan, V.S. Senthilkumar, *Procedia Engineering*, **64**, 1209-1218 (2013)

5. I.Y. Zakhariev, S.A. Aksenov, Journal of Chemical Technology and Metallurgy, **52(5)**, 1002-1007 (2017)
6. V.V. Kukhar, V.G. Artiukh, O.I. Serduik, E.Yu. Balalayeva, Procedia Engineering, **165**, 1693-1704 (2016)
7. V.V. Kukhar, Metallurgical and Mining Industry, **6**, 122-132 (2015)
8. Y. Kazashi, Journal of Computational and Applied Mathematics, **333**, 428-441 (2018)
9. M. Fuge, M.E. Yumer, G. Orbay, L.B. Kara, Computer-Aided Design, **44**, 1020-1032 (2012)
10. A.J. Sadowsky, A.M. Rotter, International Journal of Solids and Structures, **50(5)**, 781-794 (2012)
11. J. Gielis, American Journal of Botany, **90(3)**, 333-338 (2003)
12. J. Gielis, D. Caratelli, Y. Fougerolle, P.E. Ricci, I. Tavkelidze, T. Gerats, PLoS ONE, **7(9)**, e29324 (2012)
13. Y.D. Fougerolle, J. Gielis, F. Truchetet, Pattern Recognition, **46**, 2078-2091 (2013)
14. A.S. Anishchenko, A.P. Andryushchenko, Soviet Engineering Research, **5**, 54-55 (1991) (in russ.)
15. A.S. Anishchenko, Yu.V. Feofanov, A.B. Bogun, Chemical and Petroleum Engineering, **11**, 33-35 (1992) (in russ.)
16. A.S. Anishchenko, Metallography and heat treatment of metals, **2**, 31-32 (1996) (in russ.)
17. D.C. Agrawal, *Introduction to Nanoscience and Nanomaterials* (World Scientific Publishing Co. Ptc. Ltd, 2013)
18. J.-P. Lechten, J.-C. Patrat, B. Baudelet, Revue de Physique Appliquee, **12(1)**, 7-14 (1977)
19. S.A. Aksenov, E.N. Chumachenko, A.V. Kolesnikov, S.A. Osipov, Journal of Materials Processing Technology, **217**, 158-164 (2015)
20. S.A. Aksenov, E.N. Chumachenko, A.V. Kolesnikov, S. A. Osipov, Procedia Engineering, **81**, 1017-1022 (2014)
21. A.V. Grushko, V.V. Kukhar, Yu.O. Slobodyanyuk, Solid State Phenomena, **265**, 114-123 (2017)
22. V. Sikulskiy, V. Kashcheyeva, Y. Romanenkov, A. Shapoval, Eastern-European Journal of Enterprise Technologies, **4/1(88)**, 43-49 (2017)
23. V. Kukhar, E. Balalayeva, O. Nesterov, MATEC Web of Conferences, **129**, 01041 (2017)
24. E. Balalayeva, V. Artiukh, V. Kukhar, O. Tuzenko, V. Glazko, A. Prysiashnyi, V. Kankhva, Advances in Intelligent Systems and Computing, **692**, 220-235 (2018)
25. V. Kukhar, V. Artiukh, A. Butyrin, A. Prysiashnyi, Advances in Intelligent Systems and Computing, **692**, 201-211 (2018)
26. E. Asaadi, P.S. Heyns, Engineering Computations, **33(5)**, 1472-1489 (2016)
27. L. Vitu, N. Boudeau, P. Malécot, G. Michel, A. Buteri, *Comparaison de Trois Modeles Pour le Post-Traitement de Mesures Issues du Test de Gonflement Libre de Tubes* (22-ieme Congres Francais de Mecanique, Lyon), 67-78 (2015).
28. E.A. Musaev, A.E. Sheryshev, M.A. Sheryshev, Polymer Science: Series D, **10(2)**, 165-168 (2017)

29. G.C. Cornfield, R.H. Johnson, International Journal of Mechanical Science, **12(6)**, 479-490 (1970)
30. N.R. Vargasov, M.M. Radkevich, Russian Metallurgy (Metally), **2016(13)**, 1295-1297 (2016)
31. B.V. Skuridin, O.M. Smirnov, Ju.V. Gusev, O.V. Panfilova, Kuznechno-Shtampovochnoye Proizvodstvo, **12**, 35-38 (1977), in russ.
32. A.I. Rudskoy, Y.I. Rudaev, *Mechanics of dynamic superplasticity of aluminum alloy* (Sankt-Petersburg, Nauka, 2009), in russ.
33. V. Kukhar, A. Prysiazhnyi, E. Balalayeva, O. Anishchenko, Modern Electrical and Energy System (MEES), IEEE, 404-407 (2017)
34. A.R. Ragab, Metal Materials Technology, **10(1)**, 340-348 (1983)
35. V.G. Efremenko, K. Shimizu, A.P. Cheiliakh, et.al. Int. J. of Minerals, Metallurgy and Materials, **23(6)**, 645-657 (2016)
36. J. Kondratiuk, P. Kuhn, Wear, **270(11-12)**, 839-849 (2011)
37. O.M. Smirnov, V.O. Guk, M.A. Tsepin, A.S. Anishchenko, Teorya i Tehnologya Obrabotki Metallov Davleniem (Moscow, MISIS), **113**, 70-75, (1979), in russ.
38. J.J.V. Jeyasingh, G. Kothandaraman, P.P. Sinha, B.N. Rao, A.C. Reddy, Materials Science and Engineering: A, **478(1-2)**, 397-401 (2008)
39. A. Dutta, Materials Science and Engineering: A, **371(1-2)**, 79-81 (2004)
40. D.A. Kitaeva, G.E. Kodzhaspirov, Ya.I. Rudaev, In: Proceeding of the 25th International Conference on Metallurgy and Materials METAL 2016, Brno, Czech Republic, Ostrava: TANGER), 1426-1431 (2016)